Photocatalytic Activity of Phenol over Visible-light-driven Pure BiOI Nanocatalyst

Natkritta Boonprakob[1*], Janjira Tapad[1], Pongthep Jansanthea[1] and Burapat Inceesungvorn[2]

[1]Department of Chemistry, Faculty of Science and Technology, Uttaradit Rajabhat University, Uttaradit 53000, Thailand

[2]Department of Chemistry, Faculty of Science, Chiang Mai University, Chiang Mai, 50200, Thailand

***Abstract*:** *The visible-light-driven pure Bismuth oxyiodide (BiOI) nanocatalyst was successfully synthesized and obtained by coupling a homogeneous precipitation rout with solvothermal method. Photocatalytic activities of phenol over different pH suspension of BiOI samples were evaluated under visible light irradiation (λ>400 nm). The phase, crystal structure and morphology of BiOI catalyst were characterized by X-ray diffraction (XRD), scanning electron microscopy (SEM) and transmission electron microscopy (TEM). Enhanced photocatalytic activities are found from pure BiOI in all various pH suspensions of catalysts with pH 8 being the optimum condition. The promising photocatalytic activity of phenol over prepared BiOI observed in this study is ascribed mainly to its narrower band gap energy and hence increases light absorption in the visible region as evidenced by UV-vis DRS results.*

Keywords: *Phenol, Bismuth oxyiodide, Visible light, Nanocatalyst.*

1. Introduction

Nowadays, phenol and derivatives are considered to the hazardous chemical pollutants [1]. The high quantities of phenol effluent from many industries such as paints, pesticides, polymer and cosmetic production etc., have been a major cause of waste water [2–4]. In response, it has become a challenge to achieve an effective removal process of phenols from aquatic effluent to minimize the water pollution. Since the conventional processes for waste water treatment such as adsorption, reverse osmosis and ultra-filtration are either insufficient or causing secondary pollution problems therefore demands for effective, economic and environmentally non-toxic waste water [5,6]. Recently, heterogeneous photocatalysis by semiconductor has attracted considerable attention as a room-temperature process for water remediation [7]. It is the process where irradiation of a semiconductor material results in photoexcited electrons and holes which will then react with adsorbed organic contaminants to finally produce the less harmful products which are carbon dioxide and water [8,9]. Conventional photocatalyst such as modified TiO_2, ZnO, CeO_2, $BiVO_4$ have been reported the achievement of the light absorption ability to visible light region [10–13]. Recently, bismuth oxyhalides (BiOXs, X = Cl, Br, I) which is without non-titanium dioxide base have been interested [14,15]. The narrow band gap energy and strong red-shifted absorption range are the advantages parameters for the photocatalysis [16]. The narrowest band gap energy (~1.86 eV) of Pure BiOI exhibits the greatest photocatalyst among semiconductor in this family [17]. In this present work, pure BiOI nanocatalyst is synthesized by co-precipitation coupled with the solvothermal method. The photocatalytic efficiencies of pure BiOI nanocatalyst under different pH of initial supension compared with Degussa P25 are investigated by phenol degradation under visible light irradiation.

2. Experimental

2.1. Catalyst preparation

Bismuth nitrate pentahydrate ($Bi(NO_3)_3.5H_2O$), Potassium Iodide (KI), and other chemicals (AR grade) were purchased from Sigma-Aldrich and used without further purification. Pure BiOI was prepared synthesized and by coupling homogeneous co-precipitation with solvothermal techniques. Briefly, 1.092 g of $Bi(NO_3)_3.5H_2O$

was dissolved in 30 mL of absolute ethanol and stirred at room temperature until a clear solution was obtained. A certain amount of KI was then slowly dropped into the above solution, keeping Bi:I in 1:1 molar ratio. The pH was adjusted into 4.0 by ammonia solution. The mixture was transferred into PTFE bottle and then, kept at 100 °C for 6 h. After the sample cooled down, the slurry was washed by DI water for 3 times and then dried at °60 C for 12 h.

2.2. Characterization

Crystal structure of the prepared sample was examined by XRD using Rigaku MiniFlex II with Cu Kα radiation (1.541 Å). BET surface area measurement was carried out from N_2 adsorption isotherm of the sample at liquid N_2 temperature using Micromeritics Tristar 3000. The reflectance spectra (R) of the nanoparticle powders was obtained by using UV-visible diffuse reflectance spectrophotometry (UV-vis DRS) equipped with integrating sphere detector (Shimadzu, UV-3101PC). The absorption spectra were obtained by analyzing the reflectance measurement with Kubelka−Munk (KM) emission function, F(R). Optical band gap energy (E_g) can be determined from the plot between $E = 1240/\lambda_{Absorp.Edge}$ and $[F(R)h\upsilon]^{1/2}$ where E is the photonic energy in eV and hυ is the energy of an incident photon. Morphology and microstructure of the obtained catalyst was examined by a JEOL JEM-2010 SEM-EDS instrument and TECHNAI 12 Philips TEM (120 kV).

2.3. Photocatalytic Activity

Photocatalytic performance of the obtained materials under visible light (λ > 400 nm) illumination has been evaluated via phenol degradation. A 50 W Halogen lamp with an intensity of 750 W/m^2 were used as light sources. Prior to light irradiation, catalyst suspension (0.8 g/L) containing 20 ppm of phenol was stirred in the dark for 30 min to achieve adsorption-desorption equilibrium. Initial pH solution was adjusted to 3, 5, 7, 8 and 9 by adding dilute $HClO_4$ and NH_4OH, respectively. For a given time interval, the 5 mL of suspension was withdrawn and centrifuged to remove the catalyst powder. Then, the clear phenol solution was dyed according to the 4-aminoantipyrine colorimetric method (APHA, 1992) and subsequently recorded using PG90+ Instrument UV-vis spectrophotometer. For comparison, direct photolysis (without catalyst) and photocatalytic activities of the commercial TiO_2 (P25 Degussa, S_{BET} = 50.0 m^2/g) were also investigated under the same experimental condition.

3. Results and Discussion

3.1 X−ray Powder Diffraction (XRD)

Powder XRD pattern of pure BiOI sample together with standard JCPDS files are shown in Fig. 1. The diffraction peak at 2θ = 9.66º, 19.58º, 29.64º, 31.66º, 37.06º, 39.36º, 45.38º, 51.34º and 55.15º are very well corresponded to (001), (002), (102), (110), (103), (112), (004), (200), (114) and (212) crystal planes of tetragonal pure BiOI (JCPDS 10-0445) [18]. The sharp and narrowed peaks of nanocatalyst spectrum confirmed the excellent crystallized of sheet structure and also confirmed the successfully prepared in this work. According to pure BiOI (102) plane, the Scherrer's equation is calculated to the average crystallite sizes of the samples:

$$L = 0.89\lambda/\beta(\cos\theta) \quad (1)$$

where λ is the wavelength of the X-ray in nanometer (0.1541 nm), β is the width of the XRD peak at half peak-height (FWHM) in radian, θ is the angle between the incident and diffracted beams in degree, and L is the average crystallite size of the sample in nm [19]. The calculated average crystal size and specific surface area (S_{BET}) of pure BiOI photocatalysts are 26.70 nm, and 13.70 m^2/g, respectively.

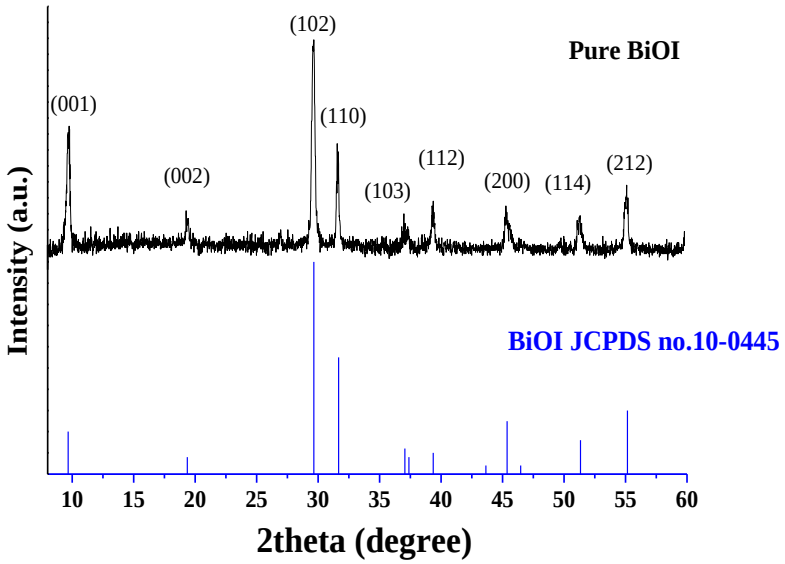

Fig. 1: X-ray diffraction patterns of pure BiOI nanocatalyst.

3.2 UV−Vis Diffuse Reflectance Spectra

UV-vis DR spectra of pure BiOI in comparison with that of Degussa P25 are shown in Figure 2(a). The optical band gap energy (E_g) could be determined by the straight-line intercept fitted to the plot in Figure 2(b). The Degussa P25 exhibits the absorption onset at 377 nm in Figure 4(a) corresponding to the band gap energy of 3.29 eV in Figure 2(b). However, the light red powder of pure BiOI is obtained. Therefore, the absorption spectrum is drastically shifted towards near the infra-red region (~608 nm) and the band gap energy is significantly narrowed to 2.04 eV in comparison with commercial TiO_2. The results suggested that pure BiOI can be photoexcited to generate more electron-hole pairs under visible-light irradiation, which could result in higher photocatalytic efficiency [20].

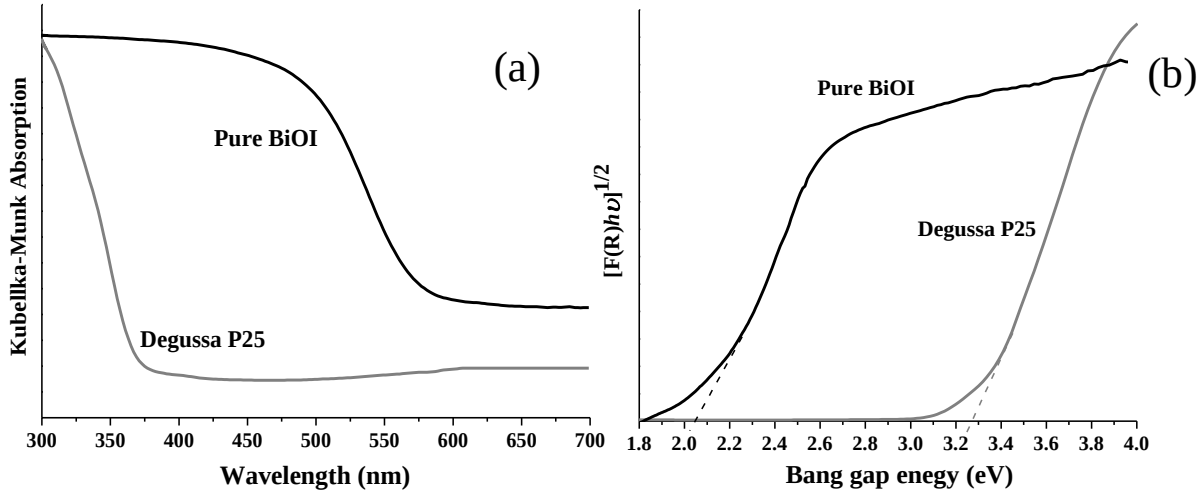

Fig. 2: (a) K-M absorbance plot and, (b) band gap energy of pure BiOI in comparison with Degussa P25.

3.3 Morphology and Microstructure

SEM micrograph (Fig. 4a) of pure BiOI exposed as the thin plate with agglomerate into the large flowerlike hierarchical structure of different size ranging from 0.9–2.0 μm. EDS spectrum of the catalyst (Fig. 4b) indicates the existence of Bi, I, and O elements in the sample. Meanwhile, TEM image in Fig. 4(c) displays 2D lamellar

structure of prepared catalyst with a diameter in the range of 15–30 nm, which aggregated in wide dimension approximately 50 nm. The average particle diameter obtained from TEM analysis is close to the value calculated from the (102) plane of X-ray diffraction peaks. The corresponding HRTEM micrograph (Fig. 4d) clearly exhibits the lattice spacing of 0.301 nm, corresponding to the (102) plane of tetragonal pure BiOI.

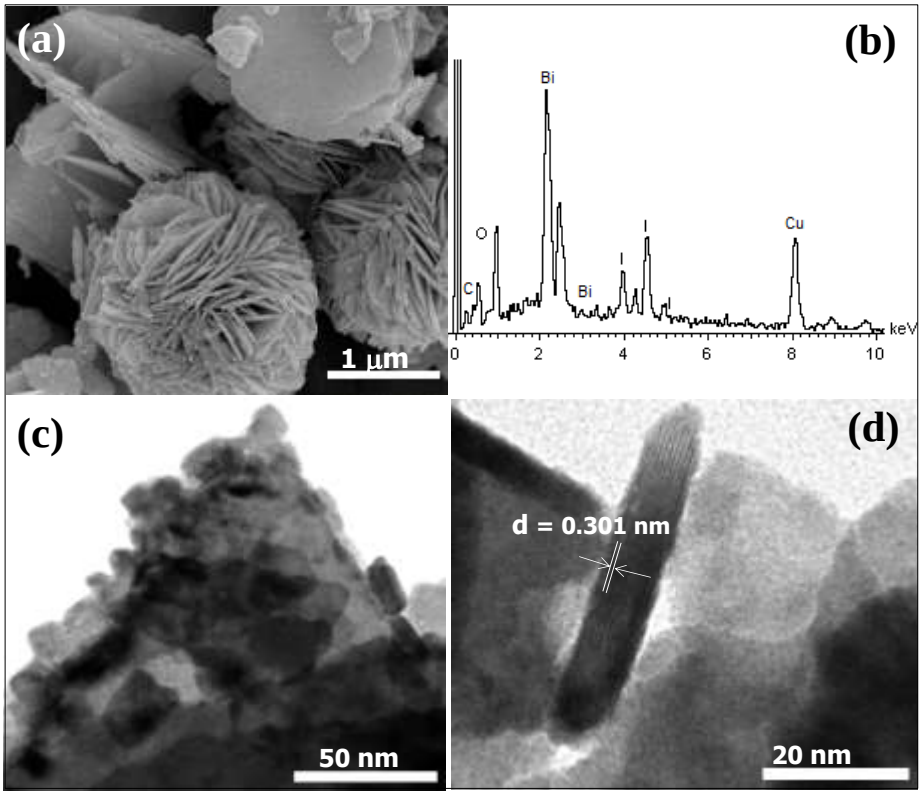

Fig. 4: (a) FE-SEM of pure BiOI, (b) EDS of pure BiOI, (c) TEM of pure BiOI, (d) TEM with lattice fringe.

3.4 Photocatalytic activities of catalyst

The photocatalytic activities of pure BiOI catalyst by phenol degradation under visible irradiation were evaluated. Phenol is the one chemical of phenolic organic compound that is often as a model pollutant to study the photocatalytic efficiency of photocatalysts. Variations of phenol concentration (C_t/C_0) versus irradiation time over the different pH of BOI catalyst suspensions are presented in Fig. 5, respectively. The pH of BiOI nanocatalyst suspension is the major parameter that affected to the photocatalytic performance because of the surface charge control of the catalysts and phenol molecule adsorption properties [21]. As a comparison, the photocatalytic activities of Degussa P25 and direct photolysis (without catalyst) were also studied at the identical conditions. The photocatalytic degradation of phenol over direct photolysis (without catalyst) could be neglected. As seen from Fig. 5, photocatalytic activities of pure BiOI catalysts exhibit significantly higher than Degussa P25. This is possibly due to an enhanced light absorption in the visible region and reduced band gap energy according to UV-vis DR study [22]. Phenol degradation activities increase when the increasing pH of suspension. The photocatalytic performance of the BiOI suspension of pH 8 is greatly similar to that of pH 9 (55% and 56%) within 7.5 h. Consequently, pH 8 is selected for the optimal experimental condition and is not necessary to use the higher pH suspension. The modified pH suspension in alkaline are ascribed more absorptivity in water media. The results also confirm that more the high alkaline pH of suspension, more hydroxide ions (OH^-). Moreover, OH^- ions could induce the generation of hydroxyl radicals ($OH^\bullet$) from oxidation reaction at the hole (h^+) on the surface of catalyst, which leading the production of strong oxidizing agent and degrade more phenol molecules [23].

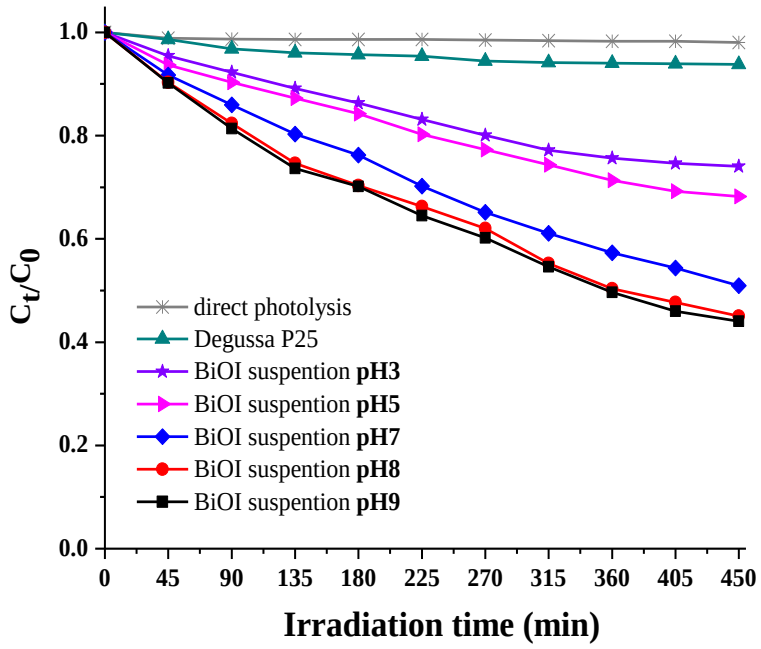

Fig. 5: Photocatalytic degradation of phenol over the different pH of BOI catalyst suspensions (initial concentration of phenol 20 mg/L and catalyst loading 0.8 g/L)

4. Conclusions

In this paper, BiOI nanocatalyst was successfully prepared by homogeneous co-precipitation coupled with a solvothermal method. The synthesis methods presented the good production of high-purity products. Photocatalytic efficiencies of BiOI in comparison with the Degussa P25 have been investigated under visible light illumination. Enhanced photocatalytic performances of BiOI can be partially ascribed to an increased light absorption in the visible region as a consequence of band gap narrowing. The pH suspension catalyst at pH 8 gives the high percentage of phenol degradation (55%) within 7.5 h with a small amount of nanocatalyst.

5. Acknowledgements

This research was financially supported by the Uttaradit Rajabhat University, Uttaradit, Thailand. In addition, this research was supported by Department of Chemistry, Department of Biology, Faculty of Science and Technology, and Science and Technology Center, Uttaradit Rajabhat University. The assistance from Paruchai Pongwan of Department of Physics and Material science, Chiang Mai University and Dr.Duangdao Channei of Department of Chemistry, Naresuan University for XRD, SEM and TEM sample preparation are also acknowledged. In addition, Dr.Boonprakob would like to thank Associated Professor Dr.Sukon Phanichphant to support Nanoscience Research Laboratory facilities.

6. References

[1] J. Matos, J. Laine, and J. Herrmann, "Synergy effect in the photocatalytic degradation of phenol on a suspended mixture of titania and activated carbon," *Appl. Catal. B: Environ.*, vol. 18, pp. 281–291, October 1998.

[2] N. Calace, E. Nardi, B. M.Petronio, and M. Pietroletti, "Adsorption of phenols by papermill sludges," *Environ. Pollut.*, vol. 118, pp. 315–319, August 2002.

[3] D. Bahnemann, "Photocatalytic water treatment: solar energy applications," *Sol. Energy*, vol. 77, pp.445– 459, November 2004.

[4] E. Grabowsk, J. R. Nask, and A. Zalesk, "Mechanism of phenol photodegradation in the presence of pure and modified-TiO_2: A review," *Water Res.*, vol. 46, pp. 5453–5471, August 2012.

[5] C. Liu, X. Liang, X. Liu, Q. Wang, N. Teng, L. Zhan, R. Zhang, W. Qiao, and L. Ling, "Wettability modification of pitch-based spherical activated carbon by air oxidation and its effects on phenol adsorption," *Appl. Surf. Sci*., vol. 254, pp. 2659–2665, February 2008.

[6] Z. Yousefi, and R. Motalebi, "Reverse osmosis in groundwater treatment for drinking water in southern Iran," *Toxicol. Lett*., vol. 189, pp. 199–203, September 2009,.

[7] T. K. Tseng, Y. S. Lin, Y. J. Chen, and H. Chu, "A Review of Photocatalysts prepared by sol-gel method for VOCs removal, *Int. J. Mol. Sci*.," vol. 11, pp. 2336–2361, May 2010.

[8] Y. Zhou, K. Vuille, A. Heel, B. Probst, R. Kontic, and G. R. Patzke, "An inorganic hydrothermal route to photocatalytically active bismuth vanadate," *Appl. Catal. A: Gen*., vol. 375, pp. 140–148, February 2010.

[9] C. H. Kwon, H. Shin, J. H. Kim, W. S. Choi, and K. H. Yoon, "Degradation of methylene blue via photocatalysis of titanium dioxide," *Mater. Chem. Phys*., vol. 86, pp. 78–82, July 2004.

[10] L. G. Devi, and K. E. Rajashekhar, "A kinetic model based on nonlinear regression analysis is proposed for the degradation of phenol under UV/solar light using nitrogen doped TiO_2," *J. Mol. Catal. A: Chem*., vol. 334, pp. 65–76, January 2011.

[11] G. S. Pozan, and A. Kambur, "Significant enhancement of photocatalytic activity over bifunctional ZnO–TiO_2 catalysts for 4-chlorophenol degradation," *Chemosphere*, vol. 105, pp. 152–159, June 2014.

[12] R. Kouraichi, J. J. Delgado, J. D. Lopez, M. Stitou, J. M. Rodriguez, and M. A. Cauqui, "Deactivation of Pt/MnOx–CeO_2 catalysts for the catalytic wet oxidation of phenol: Formation of carbonaceous deposits and leaching of manganese," *Catal. Today*, vol. 154, pp. 195–201, September 2010.

[13] S. Kohtani, J. Hiro, N. Yamamoto, A. Kudo, K. Tokumura, and R. Nakagaki, "Adsorptive and photocatalytic properties of Ag-loaded BiVO4 on the degradation of 4-n-alkylphenols under visible light irradiation," *Catal. Commun*., vol. 6, pp. 185–189, March 2005.

[14] G. Li, F. Qin, R. Wang, S. Xiao, H. Sun, and R. Chen, "BiOX (X = Cl, Br, I) nanostructures: Mannitol-mediated microwave synthesis, visible light photocatalytic performance, and Cr(VI) removal capacity," *J. Colloid Interf. Sci*., vol. 409, pp. 43–51, November 2013.

[15] Y. Zhiyong, D. Bahnemann, R. Dillert, S. Lin, and L. Liqin, "Photocatalytic degradation of azo dyes by BiOX (X = Cl, Br)," *J. Mol. Catal. A: Chem*., vol. 365, pp. 1–7, December 2012.

[16] S. Wang, L. Wang, W. Ma, D. Johnson, Y. Fang, M. Jia, and Y. Huang, "Moderate valence band of bismuth oxyhalides (BiOXs, X = Cl, Br, I) for the best photocatalytic degradation efficiency of MC-LR," *Chem. Eng. J*., vol. 259, pp. 410–416, January 2015.

[17] P. Kwolek, and K. Szaciłowski, "Photoelectrochemistry of n-type bismuth oxyiodide," *Electrochim. Acta*., vol. 104, pp. 448–453, August 2013.

[18] A. Burton, K. Ong, T. Rea, P. Ignatius, and Y. Chan, "On the estimation of average crystallite size of zeolites from the Scherrer equation: A critical evaluation of its application to zeolites with one-dimensional pore systems," *Micropr. Mesopor. Mater*., vol. 117, pp. 75–90, August 2009.

[19] S. Xie, K. Ouyangn, and X. Ma, "Low temperature synthesis of plate-like BiOIs and their highly enhanced visible light photocatalytic performance," *Ceram. Int*., vol. 40, pp. 12353–12357, April 2014.

[20] J. Su, Yang Xiao, and Mao Ren. "Direct hydrolysis synthesis of BiOI flowerlike hierarchical structures and it's photocatalytic activity under simulated sunlight irradiation," *Catal. Commun*., vol. 45, pp. 30–33, 2014, February 2012.

[21] N. Barka, I. Baka, S. Qourzal, A. Assabbane, and Y. A. Ichou, "Degradation of phenol in water by titanium dioxide photocatalysis," *Orient. J. Chem. [Online].*, vol. 29, pp. 1055–1060, June 2013.

[22] Y. Wang, K. Deng, and L. Zhang, "Visible light photocatalysis of BiOI and its photocatalytic activity enhancement by in-situ ionic liquid modification," *J. Phys. Chem. C*, 2011, vol. 115, pp. 14300–14308, June 2011.

[23] N. Wetchakun, S. Chaiwichain, B. Inceesungvorn, K. Pingmuang, S. Phanichphant, A. I. Minett, and J. Chen., "$BiVO_4/CeO_2$ nanocomposites with high visible-light-induced photocatalytic activity," *Appl. Mater. Interfaces*, vol. 4, pp. 3718–3723, June 2012.